

See discussions, stats, and author profiles for this publication at: <https://www.researchgate.net/publication/44608815>

Single-fiber grid for improved spatial resolution in distributed fiber optic sensor

Article in *Optics Letters* · May 2010

DOI: 10.1364/OL.35.001677 · Source: PubMed

CITATIONS

10

READS

79

7 authors, including:



Pandian Chelliah

Ramakrishna Mission Vivekananda College, India

32 PUBLICATIONS 110 CITATIONS

[SEE PROFILE](#)



Kasinathan Murugesan

Indira Gandhi Centre for Atomic Research

21 PUBLICATIONS 54 CITATIONS

[SEE PROFILE](#)



Sosamma Samvel

Indira Gandhi Centre for Atomic Research

25 PUBLICATIONS 83 CITATIONS

[SEE PROFILE](#)



Babu Rao Dr C

Indira Gandhi Centre for Atomic Research

102 PUBLICATIONS 554 CITATIONS

[SEE PROFILE](#)

Some of the authors of this publication are also working on these related projects:



Thermography [View project](#)



Studies on Hampi Musical Pillars [View project](#)

Single-fiber grid for improved spatial resolution in distributed fiber optic sensor

C. Pandian, M. Kasinathan, S. Sosamma, C. Babu Rao,* T. Jayakumar, N. Murali, and Baldev Raj

Indira Gandhi Centre for Atomic Research, Kalpakkam, India 603102

*Corresponding author: cbr@igcar.gov.in

Received December 21, 2009; revised March 11, 2010; accepted April 11, 2010;
posted April 19, 2010 (Doc. ID 121845); published May 11, 2010

The spatial resolution of an optical-fiber-based Raman distributed temperature sensor is limited by the pulse width of the laser used. We discuss a methodology of increasing spatial resolution by using a single-fiber grid. Spatial resolution improvement of up to 10 times is demonstrated. © 2010 Optical Society of America

OCIS codes: 060.2370, 060.2300, 120.6780.

The Raman distributed temperature sensor (RDTS) was first demonstrated by Dakin *et al.* [1]. Thirty years since, the RDTS has found wide applications such as temperature monitoring of power cables, oil and gas pipelines, and reactors [2]. The principle of the RDTS is based on optical time domain reflectometry and Raman scattering. A laser pulse is launched into the sensor fiber. The laser pulses undergo scattering. The ratio of the intensity of anti-Stokes to Stokes scattering is a measure of temperature, while the time of flight of the laser pulse gives the location of the zone where the temperature is measured [1].

The temperature measured is an integral average over the pulse width of the laser used. Thus, the laser pulse width defines the spatial resolution of the RDTS. In practice, the spatial resolution is determined by the convolution between the laser pulse characteristic, detector/receiver response, and the filter characteristics [3]. A typical RDTS, using a 5 ns pulse width laser, has a spatial resolution of 1 m. In applications such as temperature monitoring of industrial boilers, furnaces, and thermal protection systems of spacecraft, it is important that abrupt temperature variation over a small region be monitored.

Many groups have worked toward increasing the spatial resolution of the RDTS. One of the approaches is to lay the fiber in spiral mode [4]. However, this has a limitation on the minimum radius the fiber can be subjected to. Other methods are using ultrashort pulse [5], correlation [6], single-photon counting [7], and multiphoton counting techniques [8]. These methods require that either the source (the pulse width of the laser or frequency modulation of probe and pump) and/or the detector be changed.

In this Letter, an attempt at improving the spatial resolution of the RDTS is made by using a single-fiber grid (SFG). SFGs are used in geotextiles for soil monitoring [9]. The use of a SFG here is due to the consequence of weaving to integrate the single fiber in the geotextile for wider coverage rather than improving the resolution. The fiber grid was also used for physical field measurement using neural network [10]. In above cases, the fiber grid employed was not optimized for orthogonal projections. Whereas independent orthogonal projection is the basis for the

SFG proposed in our paper to improve the spatial resolution.

Here, fiber is laid along two orthogonal projections, forming a grid (Fig. 1). The advantage of this orthogonal configuration is that for a given hot spot, the temperature spread in the apparent measurement will always be along these two directions, which are mutually exclusive except at the intersection point corresponding to the location of the hot spot. The spatial resolution improvement is equal to the size of the mesh of the grid. Here we demonstrate spatial resolution improvement by 10 times.

Consider a fiber laid along two orthogonal projections as a SFG, as in Fig. 1. The size of the grid is $M \times N$, and size of the mesh is n . The arms of the grid form measuring lines, similar to projection in tomography. The bends and loops in the SFG do not participate in measurement. The fiber can be assumed to consist of discrete sections each of length equal to spatial resolution R [11]. Each section is assumed to consist of m subsections, each of length n , the size of the mesh. Thus each subsection of the grid along the x axis is represented with two indices as $S_x(i, j)$. This is interpreted as the j th subsection of the i th section along the x axis. Similarly, the m th subsection of the

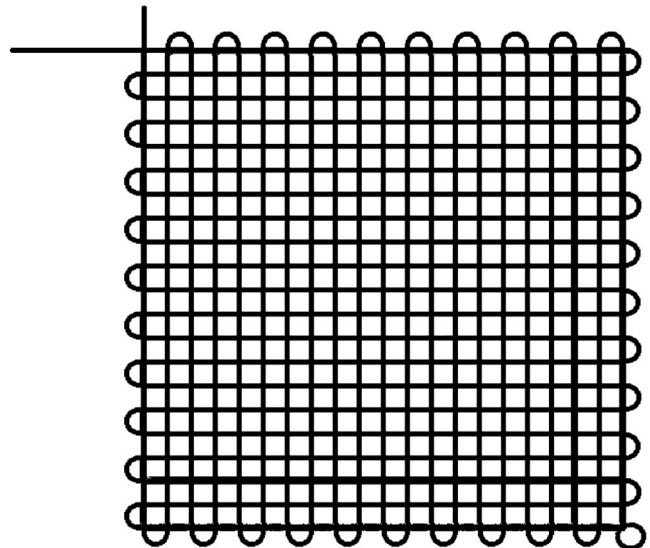


Fig. 1. SFG, 21 × 21, with mesh size 10 cm.

l th section of the y direction is represented as $S_y(l, m)$. Temperature measurement of a single subsection is represented as $T[(i, j), (l, m)]$, which has to be determined uniquely from the two orthogonal projections.

Since temperature measured in the RDTS is an integral average over the pulse width of the laser, when a single subsection $S_x(i, j)$ is heated, all the subsections belonging to section i measure the same temperature. This leads to spurious temperature points. Thus, any temperature measurement, on an SFG, is a set of true and spurious temperature measurements. Because of the mutually exclusive characteristics of the orthogonal projections of the SFG, the apparent elevated temperature of a point in one projection will not be corroborated by the measurement in other projection, except at the true measurement point. Based upon this hypothesis, it can be shown that, taking minimum of set of $\cup_i\{S_x(i, j)\}$ and $\cup_l\{S_y(l, m)\}$ reduces the number of spurious numbers considerably (Table 1).

When there is an isolated hot spot, the minimization rule identifies the true hot spot uniquely. However, if more than one hot spot is present within the same measurement zone, there still will be some spurious points left at the intersection of their projections. For a 21×21 matrix, searching the true set of measurement points involves 2^{441} combinations, roughly around 10^{130} . Having taken the minimum value for a set of two localized temperature points, the search space is limited to $2^4=16$, and for three temperature points, a maximum of $2^9=512$.

Now the problem of spatial improvement is reduced to a search problem for identification of true measurement points from a set of true and spurious points. A genetic algorithm is used to identify the true measurement points. A genetic algorithm has been used to search for an optimal solution in a much larger sample or search space. For example, for finding the optimal conformational protein structure in a protein folding problem the search space is 10^{70} [12].

Here, the set of true and spurious points $\{N_{TS}\}$ is coded as a chromosome comprising 1's and 0's. The 1 represents a true point, and 0 represents a spurious point. The length of this chromosome depends on the number of hot spots, and consequently on the number of true and spurious points. Ten such chromosomes are initialized randomly. The set of chromo-

somes constitutes a population. Each of these chromosomes represents a possible combination of $\{N_T\} \oplus \{N_S\}$.

The objective is to find the right combination, which corresponds to the actual distribution. To achieve this, for every string a localized temperature profile is reconstructed from the assumed true points (the 1's). The localized temperature T_{LR} reconstructed is compared with the temperature profile measured by RDTS, T_{SFG} . The difference between the two is the error, given by

$$\text{Error} = [(T_{LR_x} - T_{SFG_x}) + (T_{LR_y} - T_{SFG_y})]. \quad (1)$$

This has to be minimized to search for the correct chromosome.

The above proposition is tested using a 21×21 SFG, $2 \text{ m} \times 2 \text{ m}$ in size, with mesh size of 10 cm (Fig. 1). Acrylate-coated MM fiber, $50 \mu\text{m}/125 \mu\text{m}$, was used. It was also ensured that the fiber looped between adjacent measurement lines had a radius of curvature more than the minimum bending radius, 10 cm , allowed for the fiber.

The fiber was heated to 55°C in a localized zone by using a $10 \text{ cm} \times 10 \text{ cm}$ heating pad. The region corresponding to points in the grid are (10,11) and (11,12). The apparent temperature measured by the RDTS projected on the grid (Fig. 2) shows that the temperature has been underestimated. Also, this measurement has a number of spurious temperature points. By taking the minimum along the projections, the number of spurious points is brought down to two (Fig. 3). Using the methodology described in the Letter, the locations of the true temperature points, i.e., heating pads, were identified, and the temperature on the grid was reconstructed (Fig. 4). The localized heat zones can be seen more distinctively after the reconstruction. Also, the temperature reconstructed is close to the actual temperature of the heating pad.

In this Letter, we have demonstrated the improvement of spatial resolution of temperature measurement by using an SFG without modifying the optoelectronic hardware of the RDTS. The methodology was demonstrated by using multimode fiber and a RDTS. However, the methodology is also valid for single-mode fiber and other distributed fiber optic sensors such as a Brillouin optical time domain reflectometer. For ultrashort pulses, polarization-

Table 1. True and Spurious Points, before and after the Minimum is Taken along the Two Orthogonal Projections

No. of Hot Spots	No. of True Points	No. of Spurious Points ^a	No. of Spurious points after Taking Minimum
1	1	19=(2×10−1)	0
2	2	Independent hot spots 38=(2×[2×10−1])	0
2	2	Sections of hot spots overlapping at one subsection 37=(2×[2×10−1]−1)	1
2	2	Sections of hot spots intersecting at two subsections 36=(2×[2×10−1]−2)	2

^aNumber of hot spots×[number of projections×(number of subsections in a section)−number of subsections that overlap the same hot spot] − number of subsections that overlap the different hot spot.

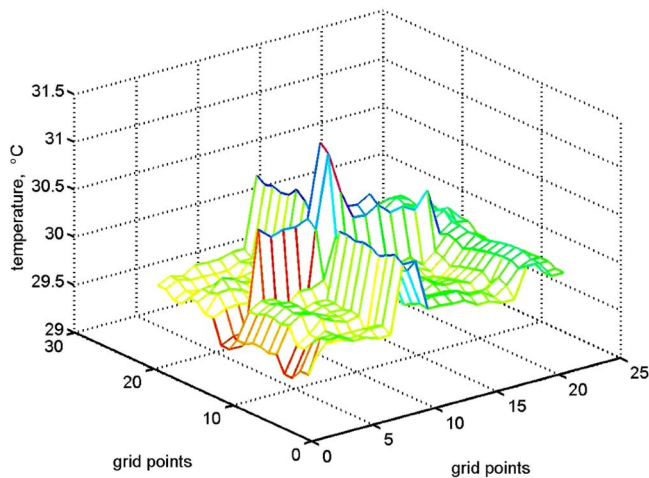


Fig. 2. (Color online) Temperature measured by RDTs projected over SFG. Note that the temperature measured by the RDTs is low compared with actual temperature.

maintaining single-mode fiber can also be used. A patent application has been submitted [13].

The authors thank Dr. P. Swaminathan, Director, Electronics and Instrumentation Group of the Indira Gandhi Centre for Atomic Research, for encouragement. The authors also thank S. Ayyappan for his help in laying the SFG. Thanks are also due to the reviewers and to Dr. Chester C. T. Shu, Topical Editor, who has helped in improving the lucidity of the paper.

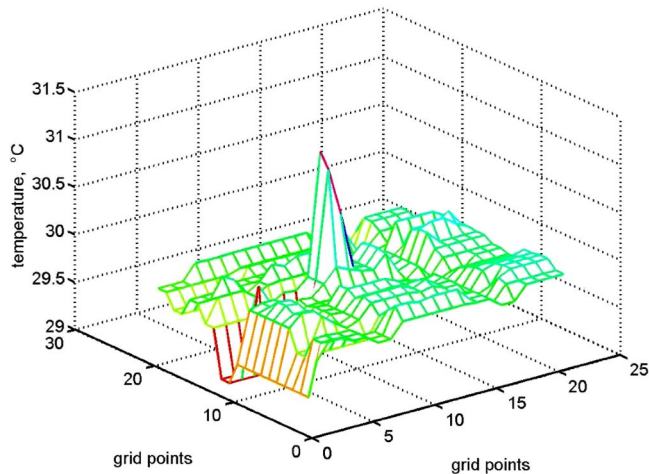


Fig. 3. (Color online) Temperature profile over SFG, after taking minimum along the two orthogonal projections.

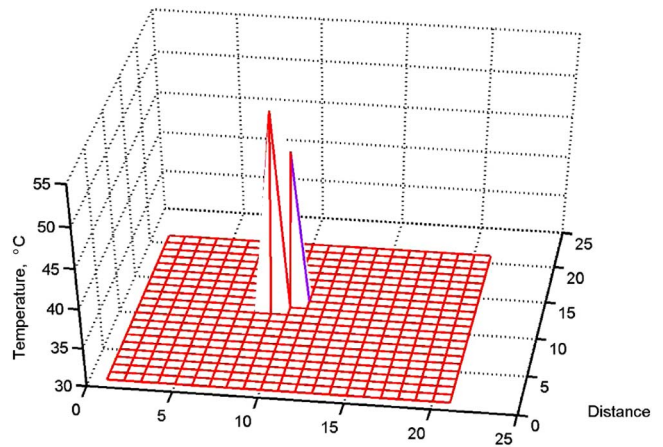


Fig. 4. (Color online) Temperature reconstructed over SFG, with improved spatial resolution. Note that the temperature reconstructed is closer to the actual temperature.

References

1. J. P. Dakin, D. J. Pratt, G. W. Bibby, and J. N. Ross, *Electron. Lett.* **21**, 569 (1985).
2. R. Berninim, A. Minardo, and L. Zeni, in *An Introduction to Optoelectronic Sensors*, G. C. Righini, A. Tajani, and A. Cutolo, eds. (World Scientific, 2009), pp. 77–94.
3. P. Healey, *J. Phys. E* **19**, 334 (1986).
4. J. P. Dakin, *J. Phys. E* **20**, 954 (1987).
5. D. A. Thorncraft, M. G. Sceats, and S. B. Pmlle, in *16th Australian Conference on Optical Fibre Technology* (Institute of Radio Electronics Engineers of Australia, 1991), pp. 183–186.
6. K. Hotate and M. Tanaka, *IEEE Photon. Technol. Lett.* **14**, 179 (2002).
7. R. Feded and M. Farhadiroushan, *IEEE Photon. Technol. Lett.* **9**, 1140 (1997).
8. M. Höbel, J. Ricka, M. Wüthrich, and T. Binkert, *Appl. Opt.* **34**, 2955 (1995).
9. B.-j. Wang, K. Li, B. Shi, and G.-q. Wei, *Landslides* **6**, 61 (2009).
10. A. V. Panov, arxiv.org, <http://arxiv.org/abs/cond-mat/0103092v1>.
11. C. Pandian, M. Kasinathan, S. Sosamma, C. Babu Rao, N. Murali, T. Jayakumar, and B. Raj, *J. Opt. Soc. Am. B* **26**, 2423 (2009).
12. J. Yadgari, A. Amir, and R. Unger, in *Proceedings of the 6th International Conference on Intelligent Systems for Molecular Biology* (AAAI Press, 1998), pp. 193–202.
13. C. Babu Rao, C. Pandian, T. Jayakumar, and B. Raj, India patent application 696/MUM/2009 A, publication July 17, 2009.